Robustness of Principal and Longitudinal Strains as Fracture Predictors in Side Impact

Damien Subit, Felix Möhler, Jacob Wass, Bengt Pipkorn

Abstract Prediction of rib fractures using computational human body models in side impact remains an elusive challenge. Although cadaveric tests carried out with extensive instrumentation (kinematics, strains) and documentation of the injuries are available, the physical characteristics of the PMHS that need to be included in a computational human body model to improve its biofidelity is still on-going. Therefore, the goal of this study was to assess the robustness of the principal and longitudinal strains as an indicator of the strain level in the ribs by running a parametric analysis where the posture of the subject and the strain measurement locations were varied. To do so, previously published side impact tests were simulated with THUMS (Total Human Body Models for Safety, v1.4), where three Post Mortem Human Subjects were postured in a nominal driving position before being struck unimpeded on the right side by a massive rigid wall travelling at 4.2 m/s. Nine models of the simulation were created to study the contribution of the posture, of the position of the arm, and of the location of the strain measurement on the ribs. The longitudinal and principal strains were computed from the simulations. It was found that the longitudinal and principal strains could be used interchangeably with THUMS, but that the predicted strains were greatly dependent on the posture and the arm angle.

Keywords longitudinal and principal strains, pre-impact posture and arm angle, side impact, strain location measurement, THUMS v1.4

I. INTRODUCTION

Anatomically detailed computational human body models (CHBM) are available for virtual testing to study complex load cases, as well as a tool for virtual prototyping of advanced restraint systems. CHBM provide a great number of measurements for each simulation which need to be properly interpreted. While the sensitivity of the simulation response to the definition of the model (geometry, material properties,…) is widely recognized and studied (e.g. [1][2][2][4]), the effect of extrinsic parameters such as the initial conditions on the injury outcome has received more limited attention [5][6]. For the thorax, rib fractures are commonly used to assess the severity of an impact in real-world crashes, in-laboratory impact and computational modeling [7][8][9]; therefore it is important for CHBM to be capable of properly predicting the number, and ideally the locations of rib fractures. However, large variations are reported in the number and location of rib fractures documented in tests performed with Post Mortem Human Subjects (PMHS). The identification of the factors that are important in the onset of fracture is an active area of research. The sensitivity of CHBM in side impact to the impact conditions has been reported in recent studies [5][6][10], where a strain threshold was used to predict fractures. Typically, the threshold is based upon the principal strains [10][11][13][14]. However, in the available experimental data obtained from tests performed with PMHS, only the longitudinal strain measured with uniaxial strain gauges along the antero-posterior direction of the rib is normally recorded [15][16][17]. Indeed, measuring the full state of strain on the rib surface thanks to multiple strain rosettes is extremely invasive [18].It is common in CHBM used in automotive safety to compare principal strains to a fracture threshold obtained from longitudinal strains measurement [10][13], as principal strains can be easily obtained from finite element simulations. The link between longitudinal strains and principal strains in the ribs during impact loadings need to be further analyzed to validate this approach.

D. S. is a Senior Researcher at the Institut de Biomécanique Humaine Georges Charpak - Arts et Metiers ParisTech (Paris, France) and a Visiting Research Professor at the Center for Applied Biomechanics - University of Virginia (USA), F.M. is a Graduate Student at Arts et Metiers ParisTech (France) and Karlsruhe Institute of Technology (Germany), J. W. is a Simulation Engineer and B. P. is the Technical Specialist & Group Leader at Autoliv Research (Sweden).

The objective of this paper was to compare the robustness of the strain level in the ribs estimated from the longitudinal strain and from the principal strains. From PMHS tests, it was shown that the strain along the rib in side impact was non-uniform [15], and that the interaction between the arm and the ribcage influenced greatly the injury outcome [17]. In the recent studies [5][6], only the effect of the change in spine curvature on the injury outcome was demonstrated with the computational model THUMS v4 (Total Human Models for Safety), as the interaction of the arm with the ribcage was not investigated.

In the current study, the side impact tests performed with PMHS [19] were simulated with the CHBM THUMS (Total Human Model for Safety, v1.4) to assess the biofidelity of the predicted strains (goal 1). Next, additional impact configurations that were closed to those evaluated in the experiments were performed to estimate the sensitivitiy of the strain prediction to the initial posture (goal 2) and the arm position and presence (goal 3). Furthermore, the sensitivity of the predicted strain to the location of the measurement along the ribs was evaluated (goal 4).

II. METHODS

Overview

Previously published side impact tests [4] were simulated with THUMS. THUMS posture was varied based on the actual posture of the PMHS [20], and the sensitivity of the strain prediction in the ribs was assessed. The simulations were run with LS-Dyna R7.1.2 (release 95028)[21], on a 16-node computing cluster. The THUMS model used in the current study is similar to that used in [22][23][24][25], except for the flesh material that was changed from a viscoelastic material to a a visco-hyperelastic material (Ogden rubber material) that yield to a lower flesh stiffness. [26] (Material card 77, with one term in the strain energy function ($W(\lambda_1,\lambda_2,\lambda_3) = \frac{\mu}{\alpha}(\lambda_1^\alpha + \lambda_2^\alpha + \lambda_3^\alpha - 3), \mu = 30\ MPa, \alpha = 20$), and relaxation function ($g(t) = Ge^{-\beta t}, G = 3000\ MPa, \beta = 310\ s^{-1}$), and the density was 0.92).

Side impact tests

The tests reported on in [19] were used as reference for the response of the human body is side impact. In these tests, three PMHS (table 1) were postured in a nominal driving position and were struck unimpeded on the right side by a massive rigid wall travelling at 4.2 m/s. The PMHS were seated on a fixed bench covered with an interface layer made of polyethylene to minimize friction between the PMHS clothing and the bench (fig. 1). The bilateral arms were cut, and the PMHS were held in position a set of tethers until a few milliseconds prior to being struck by the moving wall with a 100 mm pelvic offset.

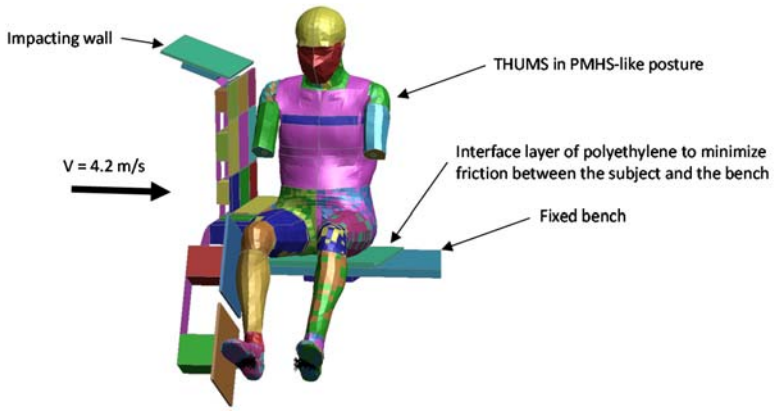

Fig. 1. Overview of the test set-up used in [19] shown with THUMS.

Extensive kinematic data was obtained from each test [20] (fig. 2). Additionally, the strain was measured in ten locations in the ribcage: two locations on ribs 4, 5, 6, 8 and 10. Out the three PMHS, the first subject sustained 16 rib fractures (right side: 3 on rib 2, 3 on rib 3, 3 on rib 4, 3 on rib 5, 1 on rib 6 and 1 on rib 7; left rib: 1 on rib 2) and a disrupted shoulder joint (tears of the coracoacromial and glenohumeral ligaments), while the two subsequent subjects sustained no injuries.

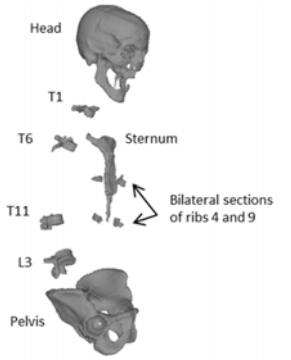

Fig. 2. Body segments for which the kinematics was measured [20].

TABLE I
SUBJECTS INFORMATION [19]

Test	1413	1414	1415
Age at time of death	67	54	71
Cause of death	Stroke	Brain aneurysm	Laryngeal cancer
Body mass (Without hand and lower arm), kg	59.9	63.1	68.9

Adjustment of THUMS posture

Adjustment of THUMS spine

THUMS' bilateral arms were cut right below the third distal part of the upper arm, similar to what was done in the experiments. Next, the posture of THUMS was modified to match that of the PMHS: posture was defined as the curvature of the spine and the position of the arm. The curvature of the spine was adjusted following the method outlined in [27] First, the position and orientation of the T1 vertebra relative to the pelvis was measured on the PMHS and normalized by the length between T1 and the pelvis. Second, the distance between the center of the T1 vertebra and the center of the pelvis measured on THUMS was used to adjust the translation of T1 based on the difference in size between THUMS and the corresponding PMHS. Third, a simulation was run to set THUMS pelvis is the position relative to T1 that matched the PMHS' posture, defined as P1, P2 and P3 (fig. 3). The arm was set at angle of 40° of shoulder extension relative to the vertical direction (see next section *Adjustment of the struck arm angle*), similar to values reported on in the experiments.

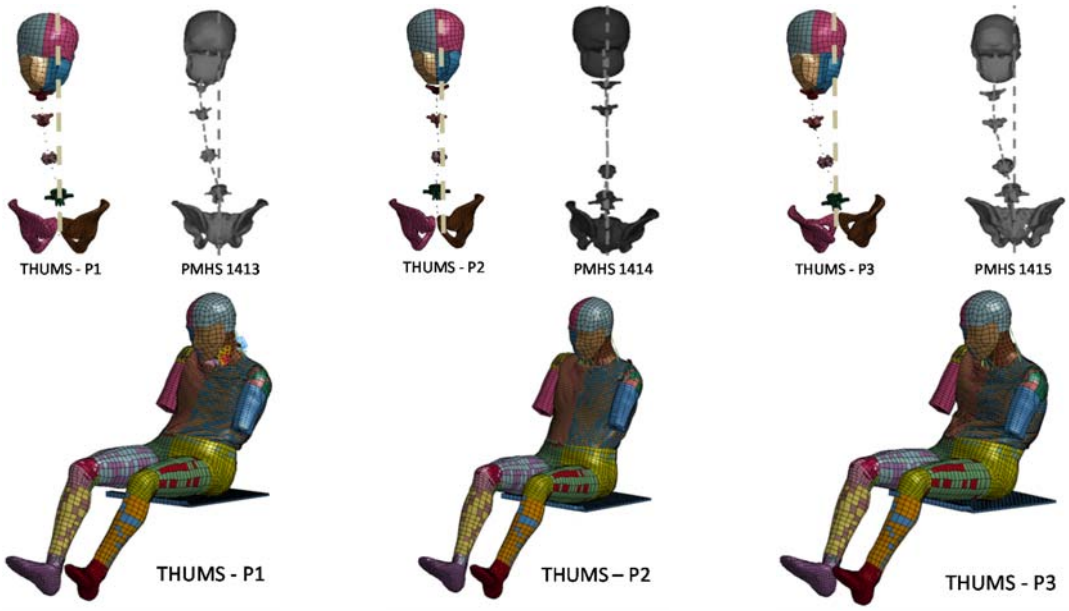

Fig. 3. THUMS in the posture matching that of the PMHS. THUMS – Px indicates the load case where THUMS spine posture matched the posture Px.

Adjustment of the struck arm angle

The shoulder joint was flexed from its position in THUMS default position to match the upper arm angle documented in the three PMHS tests (40° relative to the vertical direction). A rigid body rotation of the upper arm (humerus and surrounding flesh) was applied about the mediolateral axis in the glenohumeral joint on the struck side.in the LS-Dyna pre-processor. The mesh of the flesh around the shoulder was minimally modified to ensure adequate element quality. Three shoulder angles were created for THUMS - P3 (fig 4), as the morphology of PMHS 1415's ribcage was the closest to that of THUMS.

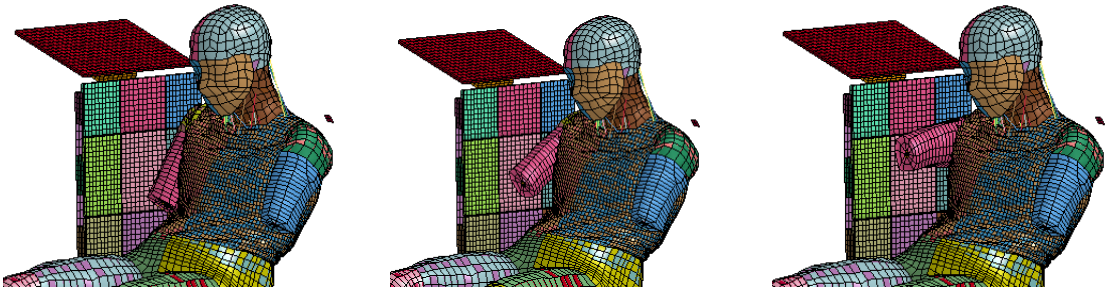

Nominal shoulder angle + 25° of extension + 50° of extension

Fig. 4. THUMS in the posture of PMHS 1415, with the struck arm in three positions.

Instrumentation of THUMS

In the experiment, the position of the strain gauges was documented for each PMHS by providing the curvilinear distance from the posterior aspect of the rib to the center of the strain gauges [19]. The normalized curvilinear position of each strain gauge was obtained by dividing the curvilinear distance from the posterior aspect of the rib to the strain gauge by the total length of the ribs. The same process was applied to THUMS rib, were the curvilinear abscissa of each element was defined as the length measured between the posterior aspect of the rib and the center of the element. The total rib length was defined as the curvilinear distance from the most anterior element to the most posterior element of the rib. All the length measurements were taken on the most lateral aspect of the rib, similar to what was done in the experiments. The principal and longitudinal strains were determined in THUMS ribs (see next section) in the locations on the ribcage similar to what was done in the experiments, namely on the anterior and lateral right ribs 4, 5, 6, and 8, and on the posterior and lateral right rib 10 (fig. 5). Three sets of strain measurement locations were created (fig. 6):

- The first set (*experiment set*) was posture-dependent, as the location of the strain measurements matched that of the PMHS reported in [19], determined by their curvilinear abscissa along the ribs.
- The second set (*normalized set*) was the same for all the posture, so as to allow for comparison between postures. The strain measurement location was the average value of the locations documented in the experiments.
- The third set (*sensitivity set*) was composed of two strain measurements per location, located 7 % of the total rib length anterior and posterior to the strain gauge locations documented in the experiments.

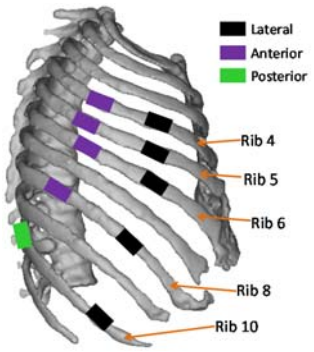

Fig. 5. Right ribcage with the nominal location of the strain gauges.

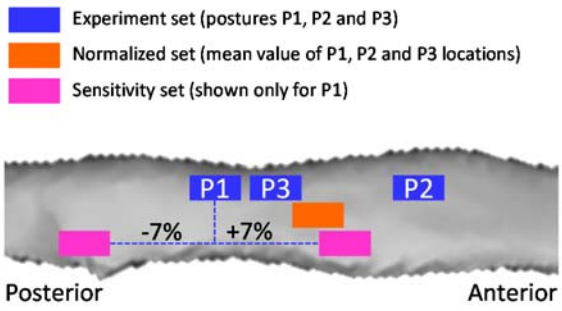

Fig. 6. Representation of the three sets of strain measurement (lateral aspect of the rib).

Rib strains measurement with THUMS

The longitudinal and principal strains were evaluated in each of the locations defined in the 3 strain measurements sets. Plane stress was assumed (per element formulation). To determine the strain in the plane of the cortical shell, the 2×2 tensor that describes the strain state in the XY plane (plane of the element) was extracted from the full strain tensor. The strain tensor and node coordinates were exported at each time and processed using a custom-made script in Matlab™ to export the longitudinal and principal strains following the methods described below.

Determination of the longitudinal strain

The strain tensor obtained for each element with Ls-Dyna is expressed in the element local coordinate system, defined based upon the position of the nodes (fig. 7): the x-axis is built upon the position of the nodes Node_1 and Node_2, and the other axis are built from there to create an orthogonal coordinate system. The node numbering in the cortical rib elements in THUMS were renumbered so that the direction defined by Node_1 and Node_2 was aligned with the rib longitudinal direction. Therefore, the strain given by the element in the first row and first column of the strain tensor (element with index (1,1)) is the longitudinal strain.

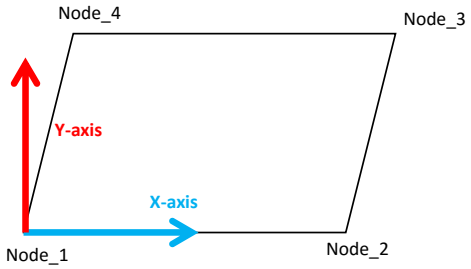

Fig. 7. Definition of the element local coordinate system in Ls-Dyna, the Z-axis is orthogonal to the X- and Y-axis, coming out of the page.

Determination of the principal strains in the cortical shell

For each time step and each of the elements in the strain gauge sets, the eigen values and eigen vectors were determined for the reduced strain tensor relative to the element coordinate system (Fig. 7). Next, the eigen values and eigen vectors were reorganized based on the sign of the eigen values and the direction of the eigen vectors so that their time history data were smooth. The major strain was defined as the maximum of the two eigen values at each time step, while the minor strain was defined as the minimum of the two eigen values at each time step. Although the major and minor strains could be directly obtained from the simulation output files, this method was used instead as it allow to estimate the orientation of the major strain axis relative to the longitudinal strain axis (the results are not presented in this paper).

Simulation matrix

The following simulation matrix was developed to answer the research question of the study (table 2). A total of nine simulations were run. For each posture:

- the configuration 'Nominal' corresponds to the simulation where both the posture and the arm position measured in the experiments are matched in the initial position in the simulations. This simulations are the closest to the experiments (E1, E2, E3),
- the configuration 'No arm contact' corresponds to the simulation where the contact definition between the arm and the thorax on the one hand, and the arm and the wall on the other hand were deleted to mimic the absence of the arm and assess how the change in posture modified THUMS impact response (E1.1, E2.1, E3.1). The position of the arm relative to the ribcage in the PMHS tests varies from subject to subject as the angle of the arm was defined based upon the horizontal direction, and not relative to landmarks on the ribcage. As a consequence, it was not possible to assess the effect of the spine posture only on the strain prediction. Therefore, as a computational work-around, the contribution of the arm was removed so as to assess how the change in spine posture affected the strain outcome.

For posture P3, three additional cases were evaluated:

- in two simulations, the shoulder on the struck side was flexed 25° and 50° from the nominal arm position (E3.2, E3.3),
- in the last simulation, the sternum and spine kinematics extracted from E3 were applied directly to THUMS while the interaction between THUMS and the impacting wall was removed.

In all the simulations, after THUMS was set in the desired posture, gravity was applied and THUMS was let settled with only the displacement in the vertical direction free (so as to keep the posture intact). Additionally for E3.2 and E3.3, the flexion of the shoulder joint was adjusted.,Finally THUMS was struck by the wall, except in E4.

The load case E4 was simulated to estimate the strain level in the ribcage generated only by the kinematics of the sternum relative to the spine, without the interaction with the arm.

TABLE 2
SIMULATIONS MATRIX

Posture	Configuration	Number of simulations
P1	E1. Nominal E1.1. No arm contact *	2
P2	E2. Nominal E2.1. No arm contact *	2
P3	E3. Nominal E3.1 No arm contact * E3.2 25° of shoulder flexion E3.3 50° of shoulder flexion E4. Controlled kinematics: the kinematics of the sternum and of the spine were extracted from E3, and applied to the sternum and the spine. The interaction with the wall was removed.	5

Data processing

The simulation data were processed and analyzed for different strain measurement sets, with different goals (Table 3). The peak strain value (longitudinal and principal strains) and the time of peak strain were estimated from all the simulation results. The longitudinal strains were compared to the corresponding experimental values. The biofidelity assessment was performed to obtain a baseline for the difference between the longitudinal strains predicted with the model and the longitudinal strains measured in the experiment, by looking at the effect of posture an arm position on the strain outcome.

When experimental data was available, the longitudinal strains were compared to the PMHS results. When no experimental data was available, only the principal strains were analyzed.

TABLE 3
ANALYSIS MATRIX

Goal	Simulations	Strain measurement sets *Strains of interest*
Biofidelity	E1, E2, E3 E3, E3.1, E3.2, E3.3	Experimental *Longitudinal strains*
Effect of spine posture	E1.1, E2.1, E3.1	Normalized *Longitudinal and principal strains*
Arm presence and position	E3, E3.1, E3.2, E3.3, E4	Normalized *Principal strains*
Sensitivity to strain measurement location	E3	Sensitivity *Longitudinal and principal strains*

III. RESULTS

For each of the four goals (Table 3), barplots that show the peak strain values and the time of peak strains for each simulation considered for that goal are presented.

Biofidelity assessment

The longitudinal strains predicted by the model at the location measured in the experiment were dependent on the posture (Fig. 8). The strains were negative in most location (compressive strain). Overall, when combining the results for the three postures, the model under predicted the measured strain in absolute value in 25 out of the 30 locations (Fig. 8a). In terms of time of the peak strain value, the model predicted a later peak value in 20 out of the 30 strain locations (Fig. 8b). The simulation with THUMS - P3 showed the best correlation with the experiments.

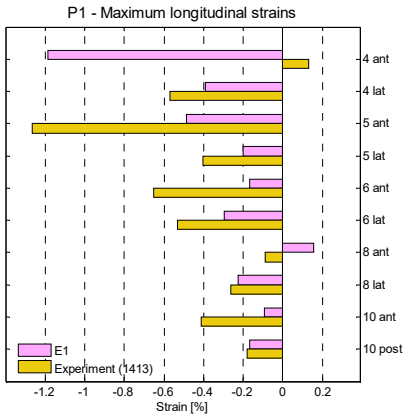

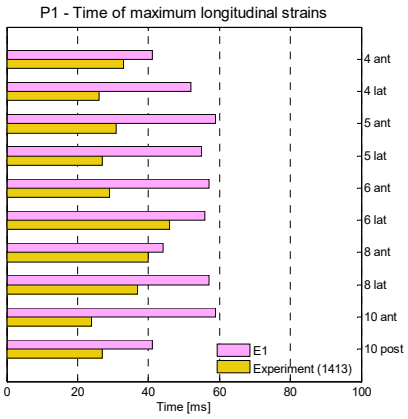

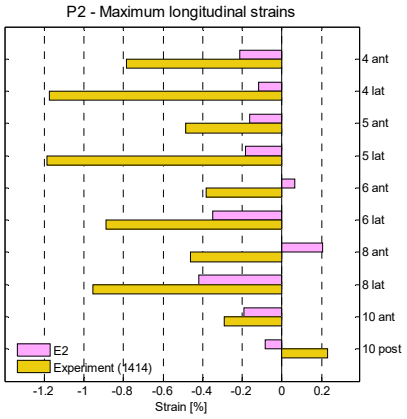

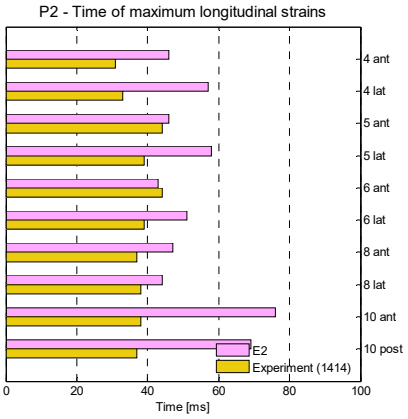

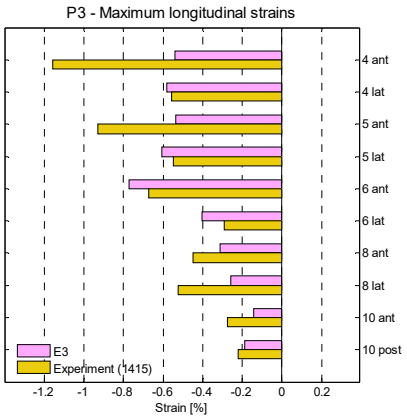

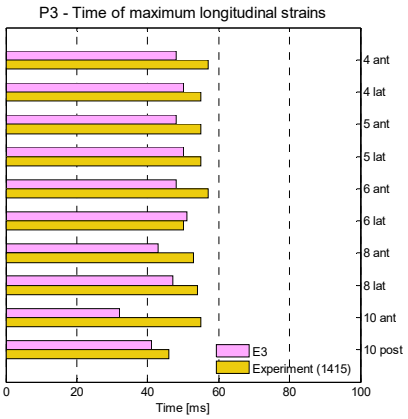

Fig. 8a. Maximum longitudinal strain (determined based on the absolute values). Strain measurement set: experiment set.

Fig. 8b. Time of peak strain. Time 0 is the time of first contact between the wall and THUMS (in the pelvis area).

The presence of the arm and its position were found to greatly affect the value or the predicted strain (Fig. 9a), while the time of peak value was less sensitive to it, except for rib 4 lateral (Fig. 9b). The closest match between the experiment and the simulation results was obtained for the arm in the nominal orientation.

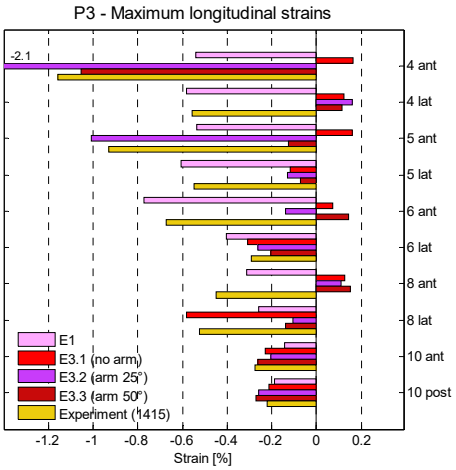

Fig. 9a. Maximum longitudinal strain (determined based on the absolute values). Strain measurement set: experiment set.

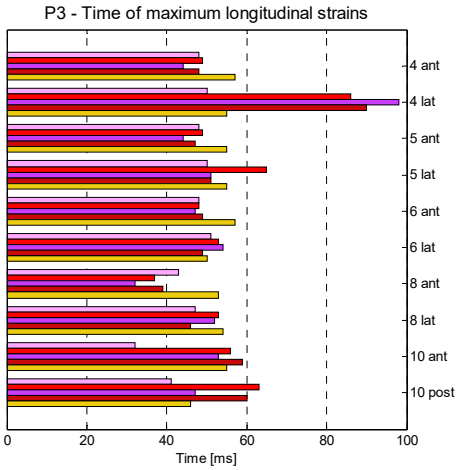

Fig. 9b. Time of peak strain.

Effect of spine posture

The peak longitudinal strains were different for each posture (Fig. 10a), and the variability in peak time was within 20 ms (Fig. 10b). For the principal strains (Fig. 11a), the variation in the predicted strains as a result of the change in posture was minimal, except for rib 8. The times of peak strain were moderately different for the minor and major strains (Fig. 11b).

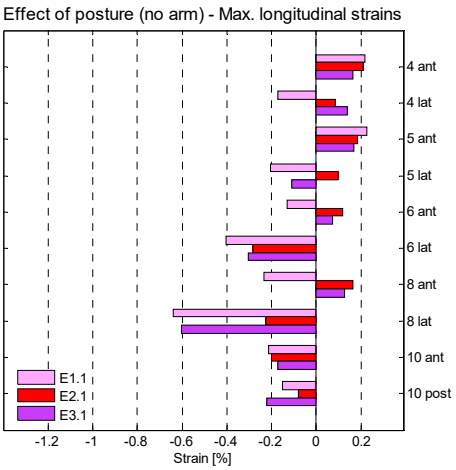

Fig. 10a. Maximum longitudinal strain (determined based on the absolute values). Strain measurement set: normalized set.

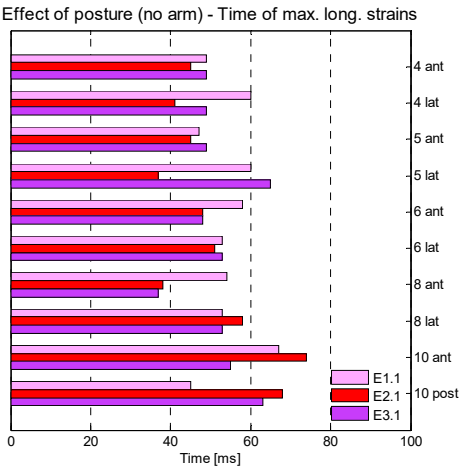

Fig. 10b. Time of peak strain.

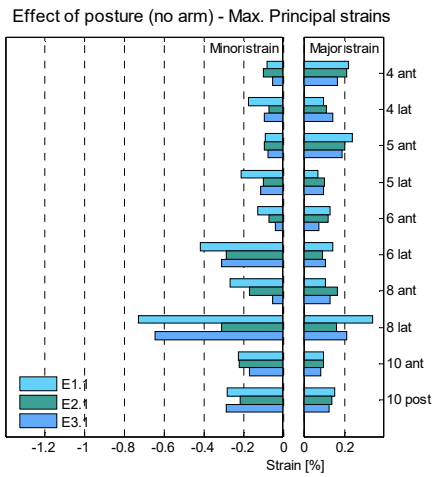

Fig. 11a. Peak principal strains. Strain measurement set: normalized set.

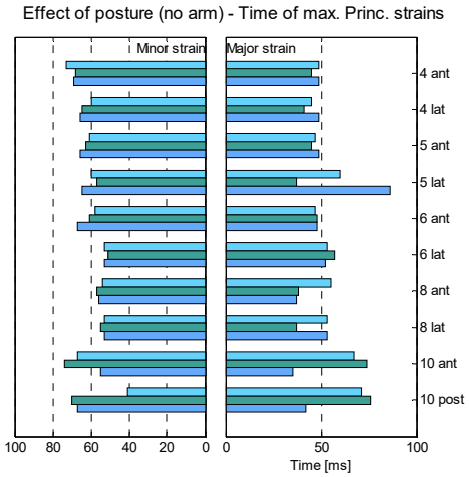

Fig. 11b. Time of peak minor and major strains.

Arm presence and position

The presence and position of the arm was found to have a significant effect on the principal strains values (Fig. 12a), while having less effect on the time of peak value, except for three outliers (lateral rib 4, 5 and 6, for the arm flexed to 50° or the controlled kinematics)(Fig. 21b).

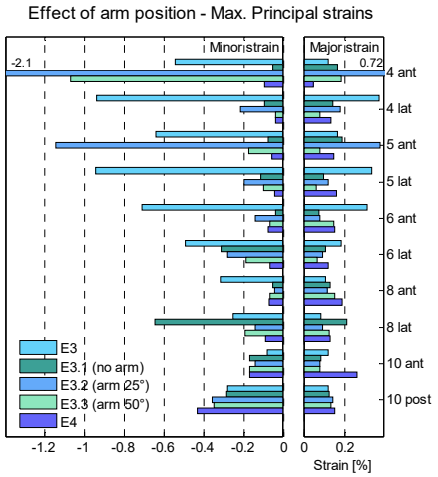

Fig 12a. Peak principal strains. Strain measurement set: normalized set.

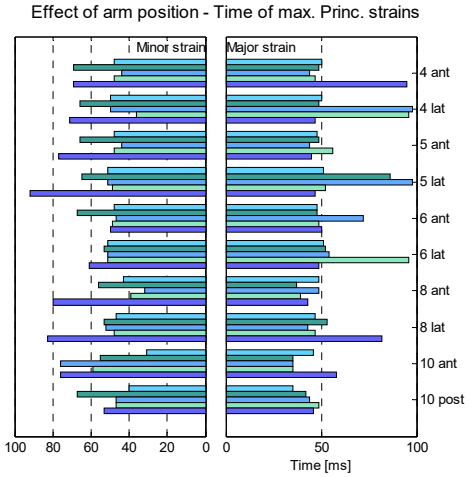

Fig. 12b. Time of peak principal strains.

Sensitivity of the strain prediction to strain gauges location

The location of the strain gauges along the rib was obtained from the PMHS. Because the size and shape of the THUMS and the PMHS ribcages are different, the sensitivity of the predicted strain to the position of the virtual strain gauges was evaluated. On average, in the experiments, the location of the strain gauges varies +/- 7 % of the rib length. It was found that a variation of 7 % in the strain gauge location (between 1.5 and 2.5 cm) could lead to an increase in the predicted strain by about 0.2 to 0.8 % (Fig. 13a). Interestingly, the time of peak value was nearly independent of the strain gauge location, except for the anterior rib 10 (Fig. 13b). Similar results were obtained for the principal strains (Fig. 14a and Fig. 14b).

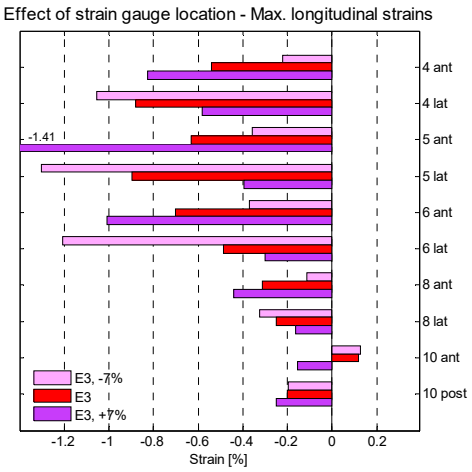

Fig 13a. Peak longitudinal strains. Strain measurement set: sensitivity set.

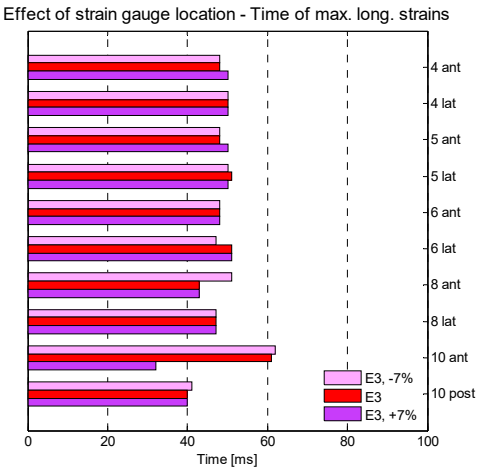

Fig. 13b. Time of peak longitudinal strains.

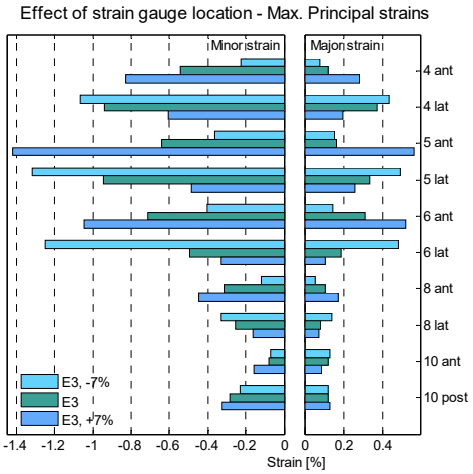

Fig. 14a. Peak principal strain. Strain measurement set: sensitivity set.

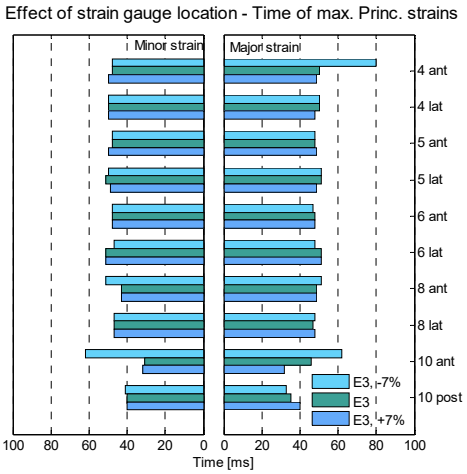

Fig. 14b. Time of peak principal strain.

IV. DISCUSSION

The response of THUMS in side impact was analyzed from several points of view: biofidelity, sensitivity to the pre-impact posture and arm presence/position, and sensitivity to the strain measurement location.

The evaluation of the biofidelity of the ribcage response at the level of the strain is a challenge that is rarely undertaken. Instead, the ribcage biofidelity is typically evaluated at the macroscopic level by using measurements such as chest deflection. Incidentally, historical studies typically provide chest deformation information obtained from chest band or video analysis [28]. Although several studies have reported analysis of real world side impact cases [29], or parametric analysis to determine the best injury predictor [10] or the sensitivity of the injury outcome to the crash characteristics [29], none of them analyzed the effect of spine posture and arm position on the injury outcome for a single crash configuration. The studies reported on in [5][6] and performed with a more recent version of the THUMS model (v4) proposed a framework to quantify the sensitivity of a CHBM to its initial posture. Several experimental studies have shown that the arm contributed to limit the strain level in the thorax when it was parallel to the thorax [17][32] or within 20° [31]. These studies do not provide sufficient information about the subject spine posture, as only the desired nominal posture is described, with no measurement of the actual subjects' posture. The study [19], combined with the kinematic analysis in [20], provides the data required to perform extensive simulation work that closely mimic the experiment set-up. In the current study, the strains predicted by the model were greatly dependent on the

change in posture (Fig. 3): in other words, this suggests that a unique individual impacted in several slightly different postures could experience different strain level in the ribcage. Although the first subject (test 1413) sustained a large number of rib fractures while the other subjects did not sustain any, the strain values predicted by THUMS - P1 are similar to those obtained with the THUMS - P2. Conversely, the strain predicted with THUMS - P3 were very close to those measured in the experiment. It is interesting to note that the biofidelity of THUMS rib strain prediction would be given significantly different ranking depending on which posture is considered or if the default THUMS posture is used. Similarly, the angle of the arm was found to play an important role in the predicted strain levels (Fig. 9a). It is consistent with [17][32], and it is interesting to note that the THUMS model used in the current study mimics this sensitivity. The simulation run without the arm interaction showed that the strain level was lower than in the simulations where the arm was present. This indicates that the direct interaction of the wall with the ribcage does not generate enough deformation of the ribcage to generate strain levels commensurate with the level observed in the experiments, at least in the upper ribcage (ribs higher than rib 6, Figs. 9a and 10a).

The influence of posture and arm interaction with the impacting wall and the ribcage is a major challenge for the development of a reliable biofidelity assessment method, as there is not enough information about the arm pre-impact position and kinematics throughout the impact (the full kinematics (translation and rotation) of the struck arm was not measured during the tests) to include this information in the simulation. What is more, the predicted strain was found to be very sensitive to the location of the strain measurement location on the rib (Fig. 13a). This result is in line with [15], where corridors where created from the strain along the rib in side impact: it was shown that the position of the peak value was dependent on the type of loading (impactor or unfolded airbag). Therefore, the location of the strain measurement, either in experiments or simulations, has to be carefully decided based on the expected type of deformation. A particularity of side impact loading is that it can generate both compressive and tensile strains on the outer surface along the rib [15], while in frontal loading the outer surface of the ribs experience almost exclusively tension [16].

In the simulation results with THUMS v1.4, the principal strains exhibited good correlations with the longitudinal strains, and therefore both strains can be used to estimate the strain level in the cortical ribs. Principal strains is commonly used in FE analysis as it is a default output of any simulation software package, while estimating the longitudinal strain requires to compute this measurement. However, this result should not be interpreted as a proof that longitudinal strains are sufficient to predict fracture. It would rather suggest that the THUMS rib models are not very sensitive to more complex (non-tensile) loadings, which is consistent with the impossibility to properly predict the location of rib fractures. This limitation is not specific to THUMS and has been reported in other computational models such as the GHBMC [33][34]. Yet, the modification of the posture and of the arm angle is not sufficient to fully characterize the differences between PMHS and the model. In particular, the geometry of the ribcage was shown to vary between people as a function of age, sex and body mass index [35] and the impact response of the thorax was found to greatly depend of the geometric properties while being less sensitive to variation in material properties [3]. The next step for the current study will be to assess how changes in the thorax geometry influence the predicted Impact response. Another topic of interest is to improve rib fracture prediction in side impact by the development of a methodology to test ribs at the component level in a configuration that is consistent with what the ribs are subjected to in side impact [37]. The initial attempt reported on in [38] showed that the rib boundary conditions in side impact had to be better understood to define a relevant test methodology.

Finally, the contribution of the scapula was not analyzed in the current study, although [20] reported large variations between the three PMHS included in the test series (position and orientation relative to the thorax). Because of the large inter-individual variations inherent to PMHS, a parametric analysis based on a computational model is a coherent approach to further investigate how the load is transmitted through the scapula and the thorax in side impact.

V. CONCLUSIONS

The THUMS computational model was used to simulate side impact tests performed with three PMHS. The spine posture and arm position measured in the experiment were used to set-up THUMS pre-impact

configurations similar to that of the PMHS. The effect of the interaction of the arm with the ribcage on the predicted strain was investigated, along with the influence of the strain measurement location in the rib FE models. It was shown that the posture and arm angle greatly influence the strain level predicted in the simulation, and therefore, the assessment of the model biofidelity requires to test several pre-impact configurations. In THUMS, the longitudinal and principal strains could be interchangeably used to assess the strain level in the ribs. This study did not include the contribution of the thorax geometry or scapula position and orientation to the impact response predicted with the computational model, but it is the next logical step.

VI. ACKNOWLEDGEMENT

The analysis performed in this study has been funded by and carried out in association with SAFER - Vehicle and Traffic Safety Centre at Chalmers University of Technology, Sweden. D. Subit thanks the European Union for its financial support through the Marie Curie International Incoming Fellowship (FP7-PEOPLE-2013-IIF, project BioAge # 622905). F. Möhler gratefully acknowledges the financial support from the Franco-German University through the Franco-German double degree program between Arts et Metiers - ParisTech and Karlsruhe Institute of Technology. The views expressed in this article are those of the authors and do not necessarily represent the views of the funding bodies.

VII. REFERENCES

[1] Ito O, Dokko Y, Ohashi K. Development of adult and elderly FE thorax skeletal models. *SAE International*l, 2009.

[2] Jacobo,A, Yamamoto Y, Kato R, Sato F, Ejima S, Dokko Y, Yasuki T. Influence of age specific parameters on the thoracic response under controlled belt loading conditions, *International Journal of Automotive Engineering*, 6(3):83-90, 2015, 10.20485/jsaeijae.6.3_83

[3] Schoell SL, Weaver AA, Vavalle NA, Stitzel JD. Age- and sex-specific thorax finite element model development and simulation. *Traffic Inj Prev.*, 2015;16 Suppl 1:S57-65

[4] Beillas P, Berthet F. Performance of a 50th percentile abdominal model for impact: effect of size and mass. *European Society of Biomechanics Conference*, 2012.

[5] Poulard D, Subit D, Donlon JP, Lessley DJ, Kim T, Park G, Kent RW. The contribution of pre-impact spine posture on human body model response in whole-body side impact. *Stapp Car Crash J.*, 2014, 58:385-422.

[6] Poulard D, Subit D, Nie B, Donlon JP, Kent RW. The contribution of pre-impact posture on restrained occupant finite element model response in frontal impact. *Traffic Inj Prev.,* 2015;16 Suppl 2:S87-95

[7] Al-Hassani A, Abdulrahman H, Afifi I, Almadani A, Al-Den A, Al-Kuwari A, Recicar J, Nabir S, Maull KI. Rib fracture patterns predict thoracic chest wall and abdominal solid organ injury. *Am Surg.,* 2010 Aug:76(8):888-91.

[8] Shweiki E, Klena J, Wood GC, Indeck M. Assessing the true risk of abdominal solid organ injury in hospitalized rib fracture patients. *J Trauma.*, 2001 Apr;50(4):684-8.

[9] Liman ST, Kuzucu A, Tastepe AI, Ulasan GN, Topcu S. Chest injury due to blunt trauma. *Eur J Cardiothorac Surg.*, 2003 Mar;23(3):374-8.

[10] Song E, Trosseille X, Baudrit P. Evaluation of thoracic deflection as an injury criterion for side impact using a finite elements thorax model. *Stapp Car Crash J.*, 2009, 53:155-91.

[11] Forman JL, Kent RW, Mroz K, Pipkorn B, Bostrom O, Segui-Gomez M. Predicting rib fracture risk with whole-body finite element models: development and preliminary evaluation of a probabilistic analytical framework. *Annals of Advances in Automotive Medicine / Annual Scientific Conference*, 2012;56:109-124.

[12] Li Z, Kindig MW, Kerrigan JR, Untaroiu CD, Subit D, Crandall JR, Kent RW. Rib fractures under anterior-posterior dynamic loads: experimental and finite-element study. *J Biomech.,* 2010;43(2):228-34. doi: 10.1016/j.jbiomech.2009.08.040.

[13] Mendoza-Vazquez M, Brolin K, Davidsson J, WismansnJ. Human rib response to different restraint systems in frontal impacts: a study using a human body model. *International Journal of Crashworthiness*,2013, 18(5).

[14] Watanabe R, Katsuhara R, Miyazaki H, Kitagawa Y, Yasuki T. Research of the relationship of pedestrian injury to collision speed, car-type, impact location and pedestrian sizes using human FE model (THUMS Version 4), *Stapp Car Crash Journal*, 2012, 56:269-321.

[15] Leport T, Baudrit P, Potier P, Trosseille X, Lecuyer E, Vallancien G. Study of rib fracture mechanisms based on the rib strain profiles in side and forward oblique impact. *Stapp Car Crash J*., 2011, 55:199-250.

[16] Trosseille X, Baudrit P, Leport T, Vallancien G. Rib cage strain pattern as a function of chest loading configuration. *Stapp Car Crash J.,* 2008, 52:205-231

[17] Kemper AR, McNally C, Kennedy EA, Manoogian SJ, Duma SM. The influence of arm position on thoracic response in side impacts. *Stapp Car Crash J.*, 2008, 52:379-420.

[18] Subit, D, Boruah, S, Forman, J, Salzar, R, Crandall, J. Strain distribution in the human ribs during antero-posterior loading, *Japanese Society of Automotive Engineers*, 2013.

[19] Lessley D, Shaw G,et al. Whole-body response to pure lateral impact*. Stapp Car Crash J.*, 2010;54:289-336.

[20] Donlon JP, Poulard D, Lessley D, Riley P, Subit D. Understanding how pre-impact posture can affect injury outcome in side impact sled tests using a new tool for visualization of cadaver kinematics. *J Biomech.*, 2015, 48(3):529-33

[21] LS-DYNA Keyword User's Manual, Volume I & II, LS-Dyna R7.1.2, Lawrence Livermore Software Technology Corporation (LSTC), 2014.

[22] Pipkorn B, Mroz K. Validation of a Human Body Model for Frontal Crash and its Use for Chest Injury Prediction. *SAE Digital Human Modeling for Design and Engineering Conference, Pittsburgh, PA*, 2008.

[23] Pipkorn B, Subit D, Donlon J-P, Sunnevang C. A computational biomechanical analysis to assess the trade-off between chest deflection and spine translation in side impact. *Ann Assoc Adv Aut Med*, 2014.

[24] Pipkorn B, Kent R. Validation of a human body thorax model and its use for force, energy and strain analysis in various loading conditions*. International Research Council on Biomechanics of Injury (IRCOBI) Conference,* 2011.

[25] Pipkorn B, lopez-Valdes F, Lundgren C, Bråse D, Sunnevång C. Innovative seat belt system for reduced chest deflection. *Proc 24th Technical Conference on Enhanced Safety of Vehicles.* 2015, Paper Number 15-0371.

[26] Engelbrektsson, K. Evaluation of material models in LS-DYNA for impact simulation of white adipose tissue. Göteborg : Chalmers University of Technology, Department of Applied Mechanics, Göteborg, Sweden, 2011, no: 2011:46

[27] Poulard D, Subit D, Donlon JP, Kent RW. Development of a computational framework to adjust the pre-impact spine posture of a whole-body model based on cadaver tests data. *J Biomech.*, 2015, 48(4):636-43.

[28] Viano DC, Lau IV, Asbury C, King AI, Begeman P. Biomechanics of the human chest, abdomen, and pelvis in lateral impact. *Accid Anal Prev*., 1989, 21(6):553-74

[29] Golman AJ, Danelson KA, Miller LE, Stitzel JD. Injury prediction in a side impact crash using human body model simulation. *Accid Anal Prev.*, 2014 Mar;64:1-8. doi: 10.1016/j.aap.2013.10.026.

[30] Golman AJ, Danelson KA, Stitzel JD. Robust human body model injury prediction in simulated side impact crashes. *Comput Methods Biomech Biomed Engin.*, 2016;19(7):717-32.

[31] Stalnaker, R.L., Tarriere, C., Fayon, A., Walfisch, G., Balthazard, M., Masset, J., Got, C., and Patel, A. Modification of part 572 dummy for lateral impact according to biomechanical data. *Proc. 23rd Stapp Car Crash Conference*, 1979, pp: 843-872. Society of Automotive Engineers, Warrendale, PA.

[32] Cesari, D., Ramet, M., and Bloch, J. Influence of arm position on thoracic injuries in side impact. *Proc. 25th Stapp Car Crash Conference*, 1981, pp:270-297. Society of Automotive Engineers, Warrendale, PA.

[33] Li Z, Kindig MW, Kerrigan JR, Untaroiu CD, Subit D, Crandall JR, Kent RW. Rib fractures under anterior-posterior dynamic loads: experimental and finite-element study. *J Biomech.*, 2010;43(2):228-34.

[34] Poulard D, Kent RW, Kindig M, Li Z, Subit D. Thoracic response targets for a computational model: a hierarchical approach to assess the biofidelity of a 50th-percentile occupant male finite element model. *J Mech Behav Biomed Mater.*, 2015 May;45:45-64. doi: 10.1016/j.jmbbm.2015.01.017. Epub 2015 Jan 31.

[35] Shi X, Cao L, Reed MP, Rupp JD, Hoff CN, Hu J. A statistical human rib cage geometry model accounting for variations by age, sex, stature and body mass index. *J Biomech.*, 2014;47(10):2277-85.

[36] D Subit, B Sandoz, J Choisne, C Amabile, C Vergari, W Skalli, S Laporte. Rib Length Variation with Age and Sex-Measurements from High-Resolution Low-Radiation X-Ray Images of Volunteer Subjects. *24th International Technical Conference on the Enhanced Safety of Vehicles (ESV)*, 2015.

[37] Subit D, Möhler F, Pipkorn B. Biofidelity corridors for sternum kinematics in low-speed side impacts. *Traffic Inj Prev.*, 2015;16 Suppl 2:S168-75

[38] del Pozo de Dios E, Kindig MW; Arregui-Dalmases C; Crandall J; Takayama S; Ejima S; Kamiji K; Yasuki T. Structural response and strain patterns of isolated ribs under lateral loading. *International Journal of Crashworthiness*, 2011, 16(2): 169-180.